

A Comparative Assessment of Surface Wind Speed and Sea Surface Temperature over the Indian Ocean by TMI, MSMR, and ERA-40

ANANT PAREKH

Theoretical Studies Division, Indian Institute of Tropical Meteorology, Pune, India

RASHMI SHARMA AND ABHIJIT SARKAR

Oceanic Sciences Division, Meteorology and Oceanography Group, Space Applications Centre, Ahmedabad, India

(Manuscript received 24 March 2005, in final form 25 September 2006)

ABSTRACT

A 2-yr (June 1999–June 2001) observation of ocean surface wind speed (SWS) and sea surface temperature (SST) derived from microwave radiometer measurements made by a multifrequency scanning microwave radiometer (MSMR) and the Tropical Rainfall Measuring Mission (TRMM) Microwave Imager (TMI) is compared with direct measurements by Indian Ocean buoys. Also, for the first time SWS and SST values of the same period obtained from 40-yr ECMWF Re-Analysis (ERA-40) have been evaluated with these buoy observations. The SWS and SST are shown to have standard deviations of 1.77 m s^{-1} and 0.60 K for TMI, 2.30 m s^{-1} and 2.0 K for MSMR, and 2.59 m s^{-1} and 0.68 K for ERA-40, respectively. Despite the fact that MSMR has a lower-frequency channel, larger values of bias and standard deviation (STD) are found compared to those of TMI. The performance of SST retrieval during the daytime is found to be better than that at nighttime. The analysis carried out for different seasons has raised an important question as to why one spaceborne instrument (TMI) yields retrievals with similar biases during both pre- and postmonsoon periods and the other (MSMR) yields drastically different results. The large bias at low wind speeds is believed to be due to the poorer sensitivity of microwave emissivity variations at low wind speeds. The extreme SWS case study (cyclonic condition) showed that satellite-retrieved SWS captured the trend and absolute magnitudes as reflected by in situ observations, while the model (ERA-40) failed to do so. This result has direct implications on the real-time application of satellite winds in monitoring extreme weather events.

1. Introduction

For diagnosing the various processes occurring at the air–sea interface and driving/assimilating ocean and atmosphere models, boundary layer parameters measured/computed by different means need to be pooled and integrated as a common dataset. This, however, is not a straightforward exercise. The in situ and space-based measurements have differing measurement integration times, time and space resolutions, and observation precisions. Because sensing mechanisms for them are based on different physical principles, very often the measurements refer to different attributes of the

same medium. The glaring example is the SST measurements by a moored buoy and microwave radiometer. While the first refers to the subsurface waters at a depth of a few meters, the latter refers to the temperature at the depth of a few millimeters. The difference between them is known to have significant diurnal, intraseasonal, and seasonal variations (Gentemann et al. 2004; Parekh et al. 2004a). This leads us to believe that the different measurements can play both complementary and supplementary roles. Their integration can be achieved after evaluating their interconsistencies and comparisons individually and with the analysis of known numerical models. Intercomparison and validation of satellite retrievals with in situ observations is also rendered complicated by several important differences between satellite and in situ measurements, for example, spatiotemporal inhomogeneity between in situ and satellite measurements, where in situ is a

Corresponding author address: Rashmi Sharma, Oceanic Sciences Division, Meteorology and Oceanography Group, Space Applications Centre, Ahmedabad 380 015, India.
E-mail: rashmi@sac.isro.gov.in

single-point average measurement while satellite observations are instantaneous measurements averaged over a large spatial footprint.

In this study, we have made an attempt to compare surface wind speed (SWS) and SST, which are prime ocean surface parameters for air–sea exchanges with in situ observations. Accurate, simultaneous, continuous, and self-consistent time series of these parameters is critical for understanding air–sea interactions. Availability of lower microwave frequencies (6.6 and 10.6 GHz) facilitates retrieval of SWS and SST even under the cloudy conditions. On board the Indian *Oceansat-1* the multi-frequency scanning microwave radiometer (MSMR) was such a sensor. Another microwave sensor, which is widely used for various oceanographic and atmospheric studies, is the Tropical Rainfall Measuring Mission (TRMM) Microwave Imager (TMI) (Kummerow et al. 1998).

We have used collocated and concurrent satellite data over the buoy locations in the North Indian Ocean (NIO) for the entire MSMR working period (June 1999 through June 2001). We also compared SST and SWS from 40-yr European Centre for Medium-Range Weather Forecasts (ECMWF) Re-Analysis (ERA-40) with NIO data buoys. These buoy data were not included in ERA-40. A season-wise performance of these data during the premonsoon (February–May), monsoon (June–September), and postmonsoon (October–January) periods has also been studied for both SWS and SST. Assessment of SST performance for day- and nighttime observations is carried out separately. To evaluate the ability of different measurement/observation systems under the higher cyclonic wind condition, we have carried out a case study for the May 2001 cyclone over the Arabian Sea.

2. Description of observation systems

a. MSMR

The Indian Space Research Organisation launched its first ocean remote sensing satellite *Oceansat-1* on 26 May 1999, carrying an MSMR and Ocean Color Monitor. It was a near-polar, sun-synchronous satellite with an inclination of 98.98° and an equatorial crossing time at 1200 LT. The altitude of the orbit is 727 km and the orbital period is ~102 min. The orbital characteristics of *Oceansat-1* results in almost global coverage, with a repeat cycle of 2 days and 80% of the entire globe being covered on any single day. It provides global microwave brightness temperature (TB) measurements at eight channels comprising 6.6-, 10.65-, 18-, and 21-GHz frequencies with dual polarizations having spatial resolutions ranging between 120 and 40 km (Misra et al.

2002) over a swath of 1360 km. MSMR was the only microwave sensor observing TB at 6.6 GHz during the time frame of 1999–2001. With this low frequency, which is both highly sensitive to surface emissivity and least affected by atmospheric constituents, it was expected to provide accurate SST. The four operational products available from MSMR are SST, SWS, integrated water vapor (IWV), and cloud liquid water (CLW). MSMR products are available in three grid sizes of 150, 75, and 50 km.

A brief description of the retrieval algorithm used for generation of MSMR geophysical data products (Gohil et al. 2000) is given below. The details of the retrieval algorithm are also given by Sharma et al. (2002). The general form of the algorithm is

$$G = C_0(\text{CSST}, \theta) + \sum_{i=1}^{i=N} C_i(\text{CSST}, \theta) \cdot f[\text{TB}_i(M, R, \theta)],$$

where CSST is the season and region specific monthly mean climatic SST and f is the function of TB specific to the month M and geophysical location R of the MSMR. Here, C_0 and C_i are the retrieval coefficients for the i th channel, TB_i is the TB of the i th channel, and N is the total number of channels used. These coefficients were derived using simulated TB (through a radiative transfer model) and simulated environmental parameters. It involved computation of (i) atmospheric absorption (Liebe 1985) for the given frequency and incidence angle of MSMR for the known atmospheric constituents, like dominant gases and hydrometeors, and (ii) ocean surface emissivity (Hollinger 1971; Stogryn 1972) for the given frequency, incidence angle, and the polarization of the MSMR for the known ocean surface physical conditions, like SST, salinity, winds, and foam (Wilheit 1979). In turn, simulation of TB needs the vertical atmospheric profiles of temperature, pressure, humidity, and cloud liquid water density. Temperature profiles were simulated using lapse rates. The pressure profiles were computed from the hydrostatic equation using the normal values at the surface. The relative humidity from the surface to the top of the atmosphere was estimated as a linear function, depending upon the SST of the region. CLW content profiles were estimated by introducing clouds of varying thickness at different altitudes and by assuming that CLW density diminishes from the freezing level to the boundaries of clouds. These simulations were carried out separately for tropical, midlatitude, and polar regions. Before retrieving the geophysical data products, the TB values were checked for their quality. The following TB values were rejected (i) if all the values were lying within 200 km from the coast (to avoid land contamination), (ii) if

the vertically polarized values for any channel were less than the horizontally polarized values, and (iii) if the high-frequency values were less than the low-frequency values, irrespective of the polarization. Also, the TB values lying outside the range of 10–279 K were not considered. The data are flagged as “bad” if the CLW and IWV are more than 80 mg cm^{-2} and 8 g cm^{-2} , respectively. These thresholds were set depending upon the simulation studies carried out by Gohil et al. (2000).

b. TMI

The Tropical Rainfall Measuring Mission was launched as a joint mission of the National Aeronautics and Space Administration (NASA) and National Space Development Agency (NASDA) in November 1997 with the TMI passive microwave radiometer. The TMI has a full suite of channels, ranging from 10.7 to 85 GHz, that is capable of giving accurate measurements of SST through clouds (Kummerow et al. 1998), facilitating an unprecedented look over the Indian Ocean (Harrison and Vecchi 2001). Remote Sensing Systems has developed a physically based algorithm by Wentz (1998) and Wentz et al. (2001) to retrieve geophysical parameters (SST, SWS, CLW, IWV, and rain rate). It has a swath of 760 km with an incident angle of 52.8° . Because of its non-sun-synchronous low-inclination orbit limited to the tropical region of the globe ($\pm 40^\circ$), it provides frequent coverage. By virtue of its low-altitude orbit up to ~ 350 km (up to August 2001, and 402 km beyond that) it has improved ground resolution ($25 \text{ km} \times 25 \text{ km}$), in comparison with other satellite missions with similar microwave sensors, by oversampling the data, although the effective field of view for 10 GHz is 63 km (Kummerow et al. 1998). The rain-sensitive channels on board TMI are used to detect rain in the radiometer field of view. When rain is detected, the SST retrieval is discarded (Wentz et al. 2000). SST retrieval relies primarily on the 10.7-GHz channel, with the other channels essentially providing corrections for the other geophysical variables. TMI also retrieves SWS using mainly the 10.7- and 37-GHz channels. For this study, daily gridded pass-to-pass version 3A TMI SST and SWS data, available online through Remote Sensing Systems (<http://www.ssmi.com/>), were used.

c. ERA-40

ECMWF provides parameters of the ocean, land, and atmosphere at different levels as model reanalysis products. Recently, they have generated ERA-40 using observed multiplatform data, including available satellite and in situ data (ERA-40 did not include MSMR and TMI data and did not assimilate Indian Ocean buoy

data, which we have used). Six-hourly reanalysis data are produced for the globe with a horizontal resolution of $2.5^\circ \times 2.5^\circ$. Zonal and meridional components of winds (at 10-m height) and “soil temperature level 1” (equivalent to the SST of the 0–7-cm ocean layer) have been extracted over the buoy locations with a temporal window of ± 1 h. This dataset was obtained from the Web site for ERA-40 data products (online at <http://www.ecmwf.int/research/era>).

d. Indian Ocean buoys

Several deep-sea and shallow-water moored buoys have been functional in the NIO since 1997 (Premkumar et al. 2000) under the National Data Buoy Program of the National Institute of Ocean Technology (NIOT) of the Department of Ocean Development, India. These buoys are providing the oceanic as well as surface atmospheric parameters in the marine environment. During the study period, five deep-sea buoys were operated. The locations of these buoys are shown in Fig. 1. No single buoy, however, acquired continuous data over the entire study period. The SST sensor is installed at ~ 3 m below the surface and the SWS sensor is at ~ 3 m above the sea surface. The reported SST and SWS are the average values of 600 samples (measurements acquired over 10 min with a sampling speed of 1 sample per second) every 3 h. Thus, eight observations in digital form are obtained every day. The stated accuracies are ± 0.1 K with a resolution of 0.01 K for SST, and $\pm 1.5\%$ full scale with a resolution of 0.07 m s^{-1} for SWS. Postcalibration and error flagging of data are carried out by the operating agency, namely, NIOT, before the buoy data are released.

3. Methodology

a. Wind transformation

Microwave radiometer-derived SWS at 10-m height relies on the measurements of sea surface roughness with the assumption that it is in equilibrium with the wind stress at the ocean surface. Surface observations, such as buoys, measure the actual SWS at the height of anemometer (in this case, 3 m above the ocean surface). The relationship between the measured SWS at a height and wind stress at the surface depends on the vertical distance and on the amount of the turbulence/stability occurring between the height of the anemometer and the ocean surface. Measured SWS at different heights would be different from each other, even under identical atmospheric conditions. Comparing satellite-derived SWS directly with buoy-measured SWS can therefore lead to large errors. In the present work, all of

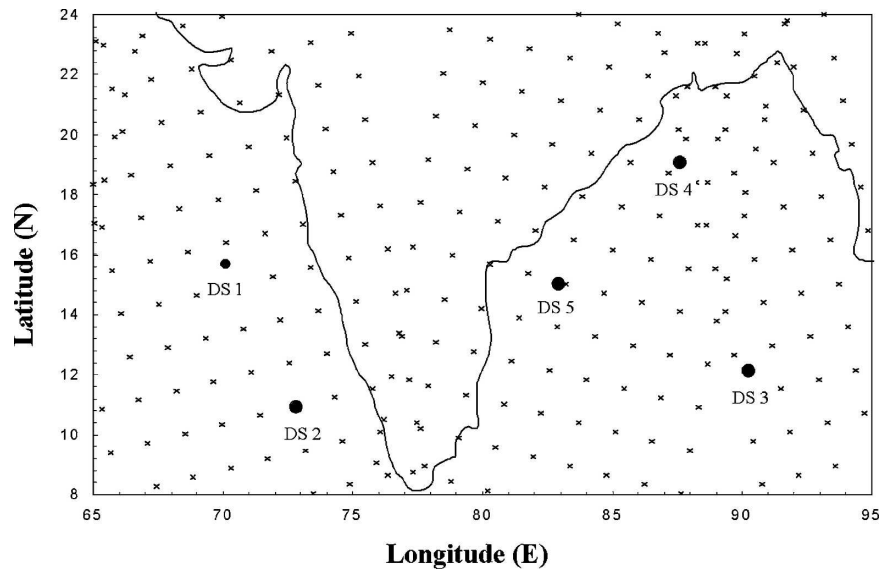


FIG. 1. Locations of NIOT deep-sea buoys with a background of MSMR daily coverage.

the buoy-measured SWS were transformed to a height of 10 m using the simple logarithmic profile approach. Mears et al. (2001) used a method that also considers the atmospheric stability while transforming winds to a different height. This method requires many atmospheric parameters, like air temperature, atmospheric pressure, and relative humidity measurements. At the buoy locations relative humidity data were not available, and hence accurate computation of stability factor was not possible. However, the differences in the two methods of transforming winds outlined above have been shown to be small (Mears et al. 2001). We therefore believe that transforming wind by making use of the logarithmic profile will not cause significant deviation from the realistic values.

b. Collocation of observations

It is necessary to develop a suitable procedure for collocating satellite observations with the in situ measurements in either space or time. There have been several studies to investigate influences of space–time window size on the satellite–in situ comparison results. While large windows are preferred for the inclusion of more collocated data in order to obtain low-variance correlation statistics, they may also introduce additional variability because of the inhomogeneous distributions of geophysical parameters (Chen and Lin 2001). Glazman and Pilorz (1990) suggest that the variations of window size (both space and time) do not have a critical impact on the accuracy of satellite–buoy comparisons. Hwang et al. (1998) suggested that time lags of up to 1 h in the case of the wind speed compari-

son do not affect the major statistics. In a more recent study by Sarkar et al. (2002), on the temporal coherence scale of wind speed over the NIO, decorrelation time was found to be about 1.5 h. Gower (1996), in his study comparing Ocean Topography Experiment (TOPEX) altimeter-derived wind speed with buoy data, emphasizes the importance of the smallest possible distances when validating sensor performance. With all of these arguments, the selection of the window for collocating satellite–in situ data will remain subjective and a compromise between the window size and the data distribution is needed.

Each MSMR pixel for SST and SWS is 150 km. Although SWS is available at a higher resolution ($0.75^\circ \times 0.75^\circ$) also, comparisons carried out earlier with limited in situ observations by Ali et al. (2000) have shown better accuracy with a 150-km grid. All of the SWS and SST observations lying within a search radius of 200 km around the buoy location and within the temporal window of ± 1 h were averaged; thus, a total of 1731 (1814) collocated pairs were generated for SST (SWS). In a similar way, collocated and concurrent pairs of TMI and buoy observations for SST and SWS within ± 1 h and a 75-km search radius were generated. Different spatial resolutions due to their orbital property (TMI is at altitude of 350 km and MSMR is at ~ 700 km) did not allow for consideration of an equal search radius for both TMI and MSMR. Also taking a 200-km search radius for TMI to make it consistent with MSMR would have resulted in additional variability because of the inhomogeneous distributions of geophysical parameters. This could have possibly resulted in incorrect

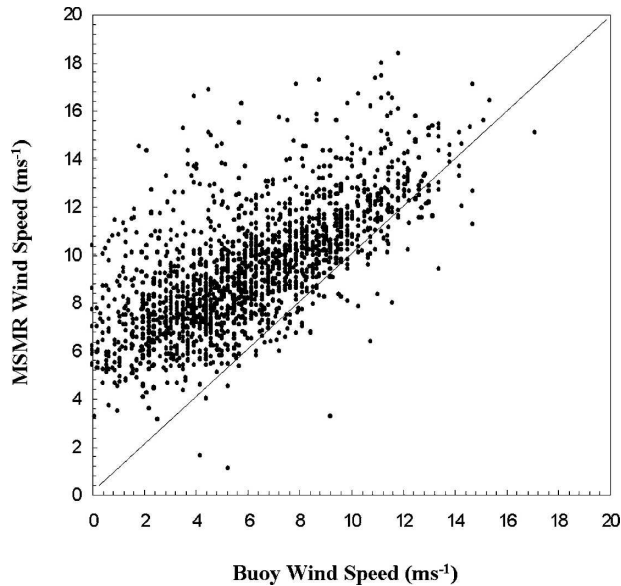


FIG. 2. Scatter analysis of MSMR-retrieved wind speed ($m s^{-1}$) and buoy-measured wind speed ($m s^{-1}$).

comparison statistics for TMI. A choice of a 75-km search radius in the case of TMI was a compromise, because a larger search radius would have resulted in additional variability and anything smaller than this would have caused untrustworthy statistics. The total number of collocated pairs for SST (SWS) is 975 (1136).

Six-hourly analyses of ERA-40 SST and SWS data available in 2.5° square grids are also used in the present study. ERA-40–buoy pairs were obtained by simply considering the nearest value of analyses to the data buoy. The number of collocated pairs of ERA-40 SST (SWS) is 3686 (3567). This number is relatively more than the satellite–buoy pairs because of the 6-hourly observations available from ERA-40.

Though the different sampling periods have been used to produce the collocated pairs with different datasets, the overall trend in accuracies is still expected to be captured. Muraleedharan et al. (2004) found that a drop in the autocorrelation coefficient for SST was marginal, even over a 24-h time window, and for SWS

it was high up to 3 h. Using the Indian Ocean data buoy observations of SWS, Sarkar et al. (2002) showed the decorrelation time to be about 1.5 h. Hence, our choice of temporal window of 1 h is expected to be appropriate.

4. Comparison with buoy SWS

The North Indian Ocean is the arena for dramatic seasonal reversal of winds. Similarly, at times, significant interannual differences are seen in the NIO. Hence, it becomes essential to compare long time series of SWS derived from satellites and model analysis fields with the observations. In this section we report detailed comparison results.

a. MSMR and buoy

A comparison of MSMR SWSs with in situ measurements from data buoys is shown in Fig. 2. The scatter diagram shows clear overestimation by MSMR for the entire range of wind speeds ($0\text{--}18 m s^{-1}$). Varma et al. (2000) found STD of the order of $2.0 m s^{-1}$ when comparing MSMR winds with the TMI observations for the first 70 days of the MSMR data. The SWS data for different ranges, namely, the low ($0\text{--}5 m s^{-1}$), moderate ($5\text{--}10 m s^{-1}$), and high ($>10 m s^{-1}$) winds, were statistically analyzed (Table 1). STD for different wind regimes ranges from 1.8 to $2.3 m s^{-1}$. The accuracies are better for moderate- and high- than for low-wind cases. The frequency distribution of winds is shown in Fig. 3 for the MSMR and buoy separately. It can be observed that the buoy-measured SWS has a range of $0\text{--}16 m s^{-1}$, whereas the MSMR SWS approximately ranges from 2 to $18 m s^{-1}$. The peaks occur at a larger value in the case of MSMR when compared with those of the buoy observations. The percentage of winds with values less than $6 m s^{-1}$ is 7% for MSMR, whereas the buoy has 30% observations falling below these values. This further supports the fact that low SWS could not be retrieved by MSMR, which may be due to the complex relation between emissivity and roughness for the low-wind cases. Winds have smaller decorrelation lengths,

TABLE 1. Comparison of SWS with buoy for different wind ranges.

Observations Wind speed range ($m s^{-1}$)	MSMR			TMI			ERA-40		
	Collocations	Bias ($m s^{-1}$)	STD ($m s^{-1}$)	Collocations	Bias ($m s^{-1}$)	STD ($m s^{-1}$)	Collocations	Bias ($m s^{-1}$)	STD ($m s^{-1}$)
0–5	727	–4.70	2.1	509	–1.67	2.78	1597	–1.55	2.65
5–10	870	–2.60	1.8	503	–0.023	1.42	1589	0.78	2.05
>10	217	–1.10	1.8	124	0.335	1.35	381	3.13	3.97
Over all	1814	–3.30	2.3	1136	–0.72	1.77	3567	–0.01	2.59

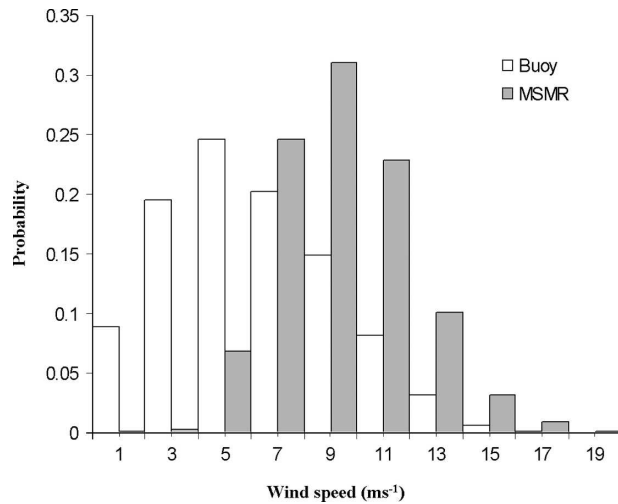


FIG. 3. Distribution of MSMR and buoy-measured wind speed (m s^{-1}) for the study period.

and hence subgrid variability could be a cause. This can also contribute to the overall statistics of MSMR SWS. To evaluate the performance under different weather conditions, statistics have been generated on seasonal scales (Table 2). The bias is largest for premonsoon and least for postmonsoon collocations.

b. TMI and buoy

The two prime frequencies for the SWS retrieval from TMI are 10.7 and 37 GHz (Wentz 1998). That the former frequency is least affected by clouds makes it an ideal channel for surface sensing. There have been several studies (Chelton et al. 2001) over the Pacific and Atlantic, reporting results of the comparison between TMI-measured SWS and those measured by a moored buoy. Time series analysis (figure not given in this paper) of TMI SWS reproduces the seasonal wind speed pattern over the NIO very well. A comparison exercise with collocated data (1136) yielded an STD of 1.77 m s^{-1} and bias of 0.72 m s^{-1} with buoy-measured SWS (Table 1). The bias found in this case is much less than that for MSMR. Senan et al. (2001) carried out a similar exercise with 3-day running average data. They found

STD ranges from 1.1 to 1.6 m s^{-1} for different buoys. Comparison of Special Sensor Microwave Imager (SSM/I) and buoy-measured wind speed over the Pacific and North Atlantic suggests that the mean difference is less than 0.5 m s^{-1} and that the STD is 1.3 m s^{-1} (Mears et al. 2001). In the case of TMI too, a relatively high STD for low SWS ($<5 \text{ m s}^{-1}$), compared to a moderate (5 to 10 m s^{-1}) and higher SWS ($>10 \text{ m s}^{-1}$), is found. Figure 4 shows a confined scatter of points except for cases of lower wind values ($<5 \text{ m s}^{-1}$), where TMI overestimates SWS. A distribution plot (Fig. 5) shows 10% of the SWS measurements $<5 \text{ m s}^{-1}$ overestimated by the TMI, which causes high STD (2.78 m s^{-1}) in the low SWS range. The retrieval of premonsoon and postmonsoon winds by TMI are exceptionally better than monsoon winds (Table 2).

c. ERA-40 and buoy

In this section we have made a detailed comparison between SWS from the atmospheric model (ERA-40) and those measured by buoys. The comparison of model SWS with buoy-measured SWS (Table 1) gives a clear overestimation (underestimation) of values by ERA-40 for lower winds (higher winds). Weller et al. (1998) had compared ERA-40 SWS with buoy observations (central Arabian Sea) and found an STD of 1.86 m s^{-1} with a mean bias 0.25 m s^{-1} . We found that the STD for winds greater than 10 m s^{-1} is very high ($\sim 4 \text{ m s}^{-1}$); overall STD for ERA-40 SWS is 2.59 m s^{-1} . Relatively poor accuracy in the present analysis as compared to that of Weller et al. (1998) could be due to the regional differences in the wind speed characteristics [a study is carried out over the NIO by Weller et al. (1998)]. The model SWSs are close to observed SWSs, during the pre- (2.32 m s^{-1}) and postmonsoon (1.94 m s^{-1}) (Table 2), rather than in the monsoon (3.42 m s^{-1}). The scatterplot of the ERA-40 and buoy SWS (Fig. 6) shows that the ERA-40 SWS has a good match for moderate SWS cases. The distribution of the two sets of SWSs (Fig. 7) shows that almost 90% of the SWS values range between 2 and 10 m s^{-1} , with the maxima around 5 m s^{-1} in the case of ERA-40.

TABLE 2. Seasonal comparison of SWS with buoy data in the north Indian Ocean.

Observations	MSMR			TMI			ERA-40		
	Collocations	Bias (m s^{-1})	STD (m s^{-1})	Collocations	Bias (m s^{-1})	STD (m s^{-1})	Collocations	Bias (m s^{-1})	STD (m s^{-1})
Premonsoon	492	-3.43	1.97	279	-0.58	1.86	810	-0.26	2.32
Monsoon	631	-2.55	2.70	351	-1.13	2.89	1155	-0.04	3.42
Postmonsoon	691	-1.14	3.12	509	-0.52	1.61	1602	0.13	1.94

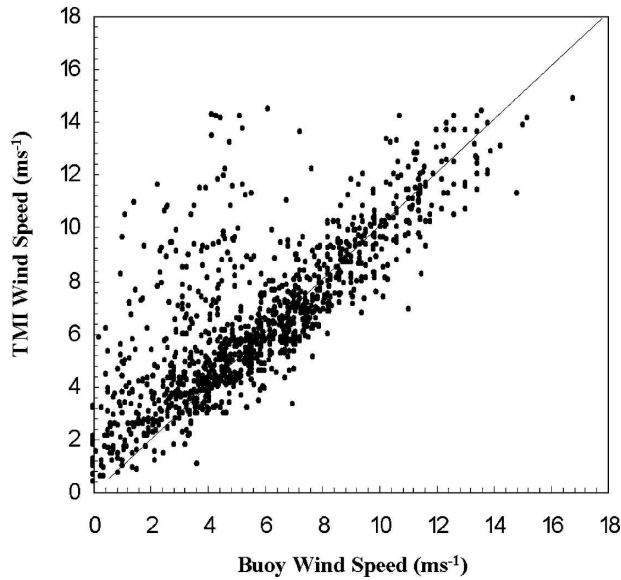


FIG. 4. Scatter analysis of TMI-retrieved wind speed (m s^{-1}) and buoy-measured wind speed (m s^{-1}).

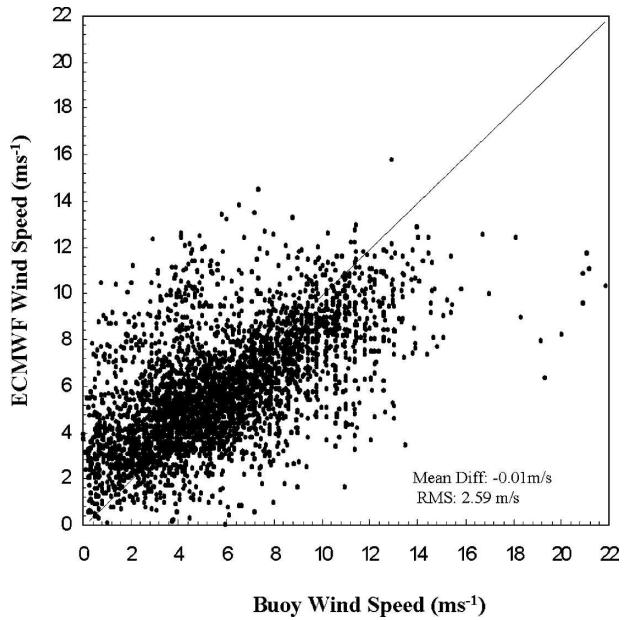


FIG. 6. Scatter analysis of ECMWF wind speed (m s^{-1}) and buoy-measured wind speed (m s^{-1}).

5. Comparisons with buoy SST

In this section the MSMR, TMI, and ERA-40 SSTs are compared with data from in situ buoys. The comparison has been carried out in two ways—by season, and day and night (separately).

a. MSMR and buoy

The time series analysis (which is not shown in this paper) of SST reveals that the fluctuations in buoy data are less than those of the MSMR SST, which show large fluctuations. This can be partially explained by the fact that the remotely sensed SST represents the tempera-

ture of the thin layer of thickness of a few millimeters or the subskin temperature (Grassl 1976), and it is known that relatively small changes in surface parameters like SWS and net heat flux can lead to changes in the subskin temperature.

Ali et al. (2000) obtained an STD of 1 K, comparing the MSMR SST with the buoy and ship observation data of 70 days. While the present study found that the STD of the MSMR SST observations ranges from 1.6 to 2.3 K with an average STD of 2.0 K and average bias of -0.67 K, the negative bias (buoy-MSMR) implies that MSMR SST is overestimated. Large STDs can be at-

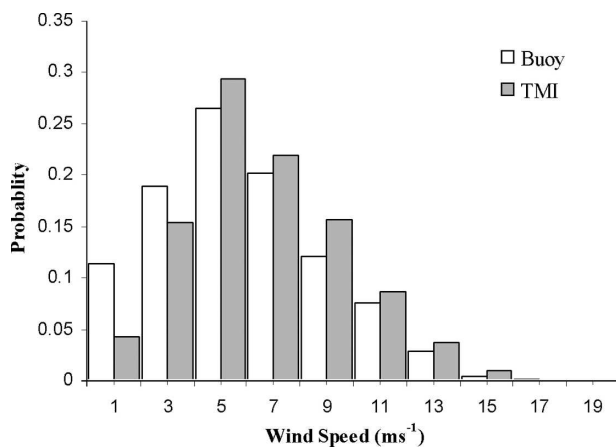


FIG. 5. Distribution of TMI and buoy-measured wind speed (m s^{-1}) for the study period.

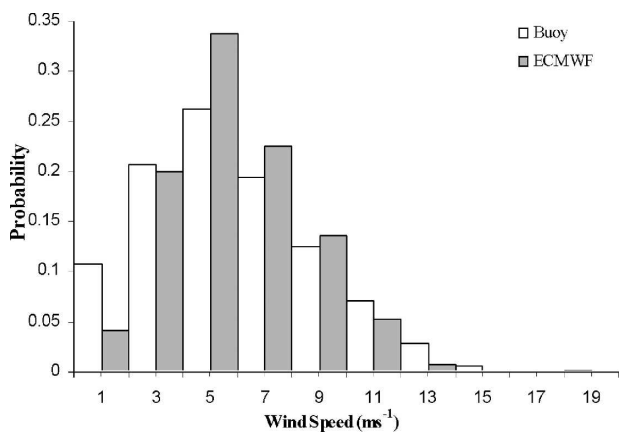


FIG. 7. Distribution of ECMWF and buoy-measured wind speed for the study period.

TABLE 3. Comparison of SST with buoy data for day and night separately.

Observation	MSMR			TMI			ERA-40		
	Collocations	Bias (K)	STD (K)	Collocations	Bias (K)	STD (K)	Collocations	Bias (K)	STD (K)
Day	762	0.00	1.6	506	-0.03	0.58	1683	-0.35	0.67
Night	969	-1.20	2.1	469	-0.18	0.61	2003	-0.46	0.69
Over all	1731	-0.67	2.0	975	-0.10	0.60	3686	-0.41	0.68

tributed to many factors, such as poor calibration, a low signal-to-noise ratio, and a larger pixel size in the case MSMR. The subpixel rain event could be another problem with MSMR. Table 3 shows that the daytime STD is 1.6 K and the nighttime STD is 2.1 K, pointing toward better performance of MSMR for the daytime than for the nighttime passes. It is interesting to see that the bias vanishes for the daytime observations, whereas it is quite high during the nighttime. Quartly et al. (2001), while comparing monthly averaged MSMR SST with TMI observations, had also reported slightly better performance of the SST retrieval for daytime radiometer passes. A seasonal comparison revealed that bias and STD are least during the monsoon season and more during the premonsoon phase (Table 4). The bias in SST could be due to the subskin and bulk temperature differences. This might be due to high winds during the monsoon producing a well-mixed upper layer of the ocean. Hence, the subskin–bulk temperature differences are less. Prior to a monsoon, low winds and clear-sky insolation lead to a thermal stratification of more than 1 K (Price et al. 1986; Schlüssel et al. 1990). Thus, large bias during the premonsoon phase can be attributed to the decoupling of the subskin and bulk layer through thermal stratification. Other possible reasons could be spatiotemporal mismatch between buoy and MSMR observations and uncertainties in the surface roughness corrections. In Fig. 8, we show the distribution of buoy minus MSMR SSTs for day- and nighttime observations separately. About 20% of the night observations ($T_{\text{Buoy}} - T_{\text{MSMR}}$) have values greater than 1.5 K, while for the daytime it is 10%.

b. TMI and buoy

Figures 9a and 9b show the comparison of TMI SST against observed SST for day and night separately. It clearly shows that TMI SST has good match up with in situ measurements. The total collocations for day (night) are 506 (469), over all STDs they are 0.6 K (Table 3) with a bias of 0.1 K, which is consistent with earlier comparison studies by Senan et al. (2001), Parekh et al. (2004a), and Bhat et al. (2004). These results also support TMI comparisons with the Tropical Atmosphere–Ocean/Triangle Trans-Ocean Buoy Network (TAO/TRITON)-, National Data Buoy Center (NDBC)-, and Pilot Research Moored Array in the Tropical Atlantic (PIRATA)-measured SST over the Atlantic and Pacific (Gentemann et al. 2004). Table 4 shows season-wise performance of TMI-retrieved SST with in situ measurements. TMI is warmer by 0.3 K when compared against buoy data for the premonsoon period, which is known for low wind and high solar insolation. However, no bias is observed in the data for the monsoon period, and the reason therefore can be attributed to high-wind conditions, which cause turbulent mixing, resulting in a homogeneous upper ocean, which is known as a well-mixed ocean. Gentemann et al. (2004) reported that 10.7-GHz TB has a weak nonlinear response to SST for the SWS greater than 12 m s⁻¹. However, it can be seen that this issue is not very serious because just 5% of the TMI SWS observations are greater than 12 m s⁻¹. Findings of the present study demonstrate the TMI's ability to measure SST under cloudy conditions as unprecedented, which is in accordance with the results of Sengupta et al. (2001), Vecchi

TABLE 4. Seasonal comparison of SST with buoy data in the north Indian Ocean.

Observations	MSMR			TMI			ERA-40			
	SST (K)	Collocations	Bias (K)	STD (K)	Collocations	Bias (K)	STD (K)	Collocations	Bias (K)	STD (K)
Premonsoon		455	1.54	2.37	261	-0.32	0.65	827	-0.63	0.88
Monsoon		561	-0.79	1.54	271	0.00	0.58	1471	-0.26	0.58
Postmonsoon		711	1.18	1.96	446	-0.03	0.57	1796	-0.27	0.59

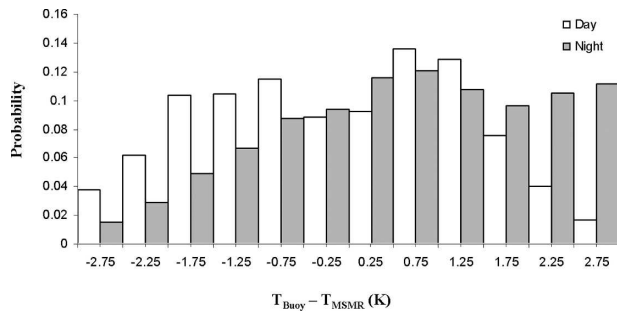


FIG. 8. Distribution of the difference between buoy-measured temperature and MSMR-retrieved temperature.

and Harrison (2002), Sarkar et al. (2004), and Bhat et al. (2004). Figure 10 shows the $T_{\text{Buoy}} - T_{\text{TMI}}$ distribution, with 90% thereof falling within a 1-K difference.

c. ERA-40 and buoy

ERA-40 provides SST every 6 h, and buoy-measured SST is available at 3-hourly intervals. This has provided the highest collocations (3686) between ERA-40 and in situ observations. Weller et al. (1998) made the comparison of ERA-40 winds with Woods Hole Oceanographic Institution (WHOI) buoy measurements during the period from October 1994 to October 1995, over the western Arabian Sea. They found a cool bias of 0.05 K with a 0.50-K STD, while in the present study bias is found to be 0.41 K and STD is 0.68 K. The larger bias found in our case could be because of the difference in the depths at which the first temperature sensor is installed in the buoy (for WHOI buoy it is at 0.17 m, whereas for Indian Ocean data buoy it is at 3.5 m). Another reason could be differences in the regional processes, which would have resulted in a cool bias. Figures 11a and 11b show the comparison between

ERA-40 and in situ observations for day and night, respectively. ERA-40 daytime SST performs slightly better than the nighttime SST. ERA-40 has a low bias and STD (Table 4) for monsoon months, while it has a large bias (warmer by 0.6 K) and STD for the premonsoon period, which could be due to upper-ocean thermal stratification, resulting from low winds and high insolation. Parekh et al. (2004b) found that the difference in warming between the 0.17- and 3.5-m depths over the western Arabian Sea can go up to 2.2 K during the premonsoon period. The statistical distribution for the temperature difference (buoy – ERA-40) shows in Fig. 12 that more than 80% of observations fall in the range from –1 to 1 K. It is also shown that about 10% of the observations of ERA-40 are warmer than 1 K with respect to the buoy for nighttime observations.

6. Cyclone case study

To assess the capability of radiometers (TMI and MSMR) and ERA-40 winds to capture cyclonic events, we have considered a case study in the Arabian Sea during 21–28 May 2001. On 24 May the cyclone was very near to the DS1 buoy location. To evaluate the performance of SWS in such extreme cases, we looked into daily averaged data around the buoy location and plotted it as a time series from 15 to 31 May 2001 (Fig. 13). The time series show a close match of the radiometers’ winds with the buoy observations. It can be seen that the TMI and the MSMR (there was a 1-day gap in MSMR data because of heavy rain) have captured severe cyclonic winds ($>20 \text{ m s}^{-1}$) as reflected by buoy winds, consistent with the findings of Parekh et al. (2002). ERA-40 winds do not reproduce the high ($>12 \text{ m s}^{-1}$) in the winds associated with the cyclone. It has underestimated the wind speed with respect to in situ

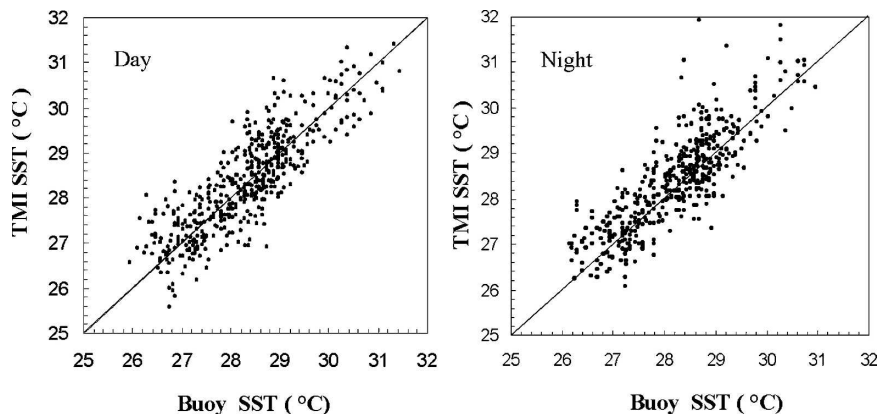


FIG. 9. Scatterplot of TMI and buoy-measured SST (K) for (a) daytime and (b) nighttime.

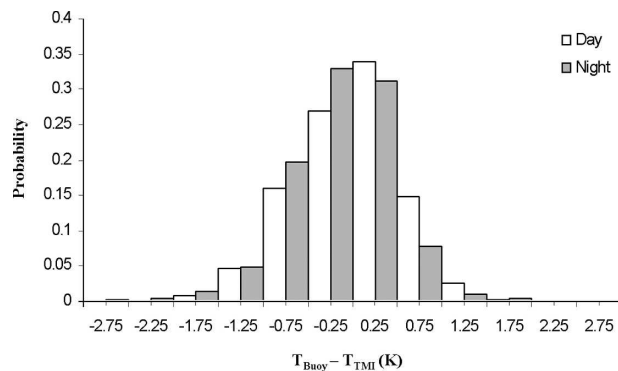


FIG. 10. Distribution of the difference between buoy-measured temperature and TMI-retrieved SST.

and satellite measurements. Because we are referring to the cyclonic conditions with respect to the surface winds, it would be quite appropriate to look at the SST variations. It is expected that under such situations, SST should be cool. A fall of 3–4 K in SST was seen in TMI, whereas the same was missing from the MSMR measurements. This could be because the retrieval algorithm of MSMR uses 6 GHz for the SST derivation, which might be more affected by the increasing winds, which roughens the ocean surface, causing complexity in emissivity.

7. Discussion and conclusions

Analysis of surface winds and sea surface temperature observations made over the North Indian Ocean by two experimental spaceborne sensors brought out their strengths and limitations. The widely used ERA-40 model analysis was also considered in our study to explore either its sufficiency or inadequacy in severe

weather cases (such as a cyclone). The two SWS and SST parameters from radiometers (TMI and MSMR) and the numerical weather prediction model (ERA-40) were compared with Indian Ocean buoy observations from both the Arabian Sea and Bay of Bengal. The satellite–buoy and model–buoy differences might arise from measurement errors in the two systems, and also from spatiotemporal sampling.

Observed biases for surface wind and SST for MSMR are large compared to TMI. This can be explained partly with respect to the radiometric resolution of the two systems—0.3 K in the case of TMI (Kummerow et al. 1998) and more than 0.6 K for the MSMR (Misra et al. 2002). Another reason could be subgrid-scale variability of the parameters resulting from a bigger footprint in the case of MSMR. An important finding has been the presence of larger biases for SST between the data (MSMR, TMI, and ERA-40) and observations for the nighttime collocations. SST from TMI, MSMR, and ERA-40 compare well with buoys under strong-wind conditions. This could be due to the turbulent mixing caused by strong winds and the consequent reduction of the difference between subskin and bulk ocean temperature, leading to a better SST comparison.

It is seen that surface wind speed is determined quite satisfactory by both TMI and MSMR (which needed a bias correction). TMI provides more accurate wind speed than ERA-40 when compared to the buoy. Overall, winds from all the three systems (TMI, MSMR, and the model) are higher than those observed at the buoy sites.

Both TMI and MSMR reproduced the winds around an Indian Ocean cyclone much better than the model analysis, justifying their inclusion in the generation of forecasting and analysis systems in the future. However, the ERA-40 winds failed to reproduce the peak in

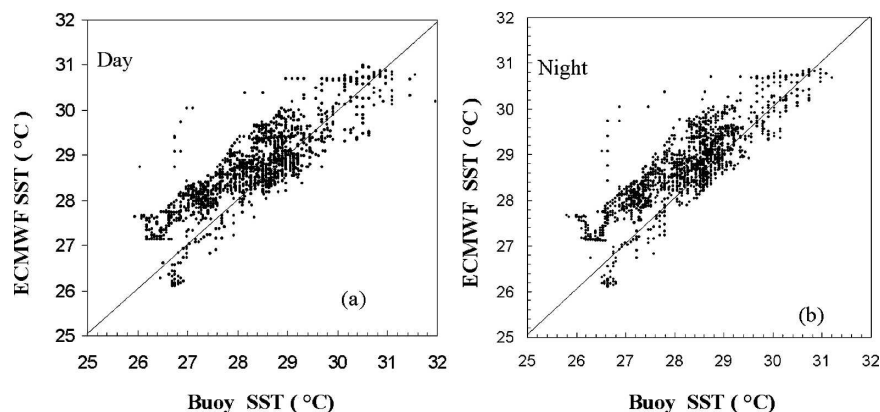


FIG. 11. Scatterplot of ECMWF and buoy-measured SST (K) for (a) daytime and (b) nighttime.

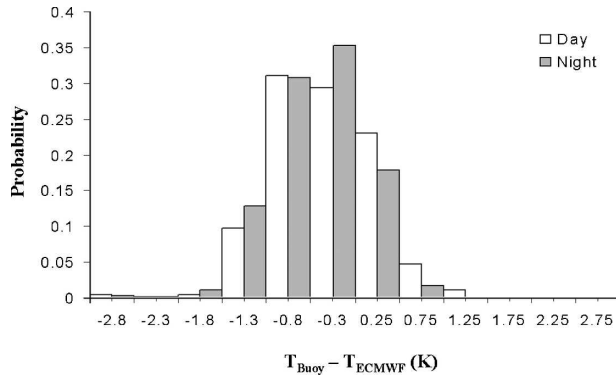


FIG. 12. Distribution of difference between buoy-measured temperature and ECMWF SST.

the cyclonic wind speed. The cyclonic activity is expected to cool down the SST because of turbulent mixing in the upper layer of the ocean. Out of the three systems, only TMI retrieved the SST-reproduced systematic cooling trend of the order of 3–4 K in a span of 2–3 days. MSMR SST failed to show any systematic cooling. Hence, MSMR-derived SSTs cannot qualify the same status. Yet, it is found to be reasonably good at reproducing synoptically averaged fields.

Though there were inherent deficiencies in the case of the MSMR, like poor calibration and radiometric resolution, a larger footprint size, and the absence of a higher-frequency channel to account for atmospheric attenuation resulting from rain and aerosols, this investigation has been a learning experience for Indian researchers. It has given an impetus and created a readiness for the Indian space community in association with Centre National d’Etudes Spatiales (CNES) of France

to launch another radiometric mission called Megha-Tropiques.

Acknowledgments. Authors are grateful to the director of the Space Applications Centre (SAC) in Ahmedabad, the director of the Indian Institute of Tropical Meteorology in Pune, and the group director of the Meteorology and Oceanography Group, SAC, for their encouragement. We would like to express our sincere appreciation to Dr. B. S. Gohil for many illuminating discussions. We especially thank two anonymous reviewers for their comments, which helped us to make significant improvements in the manuscript. Buoy observations were obtained from National Institute of Ocean Technology, Chennai. We also acknowledge Remote Sensing System and ECMWF for providing their data product.

REFERENCES

Ali, M. M., and Coauthors, 2000: Validation of MSMR geophysical parameter data products with in situ observations. *Proc. Fifth Pacific Ocean Remote Sensing Conf. (PORSEC 2000)*, Goa, India, NIO, 182–191.

Bhat, G. S., G. A. Vecchi, and S. Gadgil, 2004: Sea surface temperature of the Bay of Bengal derived from TRMM Microwave Imager. *J. Atmos. Oceanic Technol.*, **21**, 1283–1290.

Chelton, D., and Coauthors, 2001: Observations of coupling between surface wind stress and sea surface temperature in the eastern tropical Pacific. *J. Climate*, **14**, 1479–1498.

Chen, G., and H. Lin, 2001: Impacts of collocation window on the accuracy of altimeter/buoy wind-speed comparison—A simulation study. *Int. J. Remote Sens.*, **22**, 35–44.

Gentemann, C. L., F. J. Wentz, C. A. Mears, and D. K. Smith, 2004: In situ validation of Tropical Rainfall Measuring Mission microwave sea surface temperatures. *J. Geophys. Res.*, **109**, C04021, doi:10.1029/2003JC002092.

Glazman, R. E., and S. H. Pilorz, 1990: Effects of sea maturity on

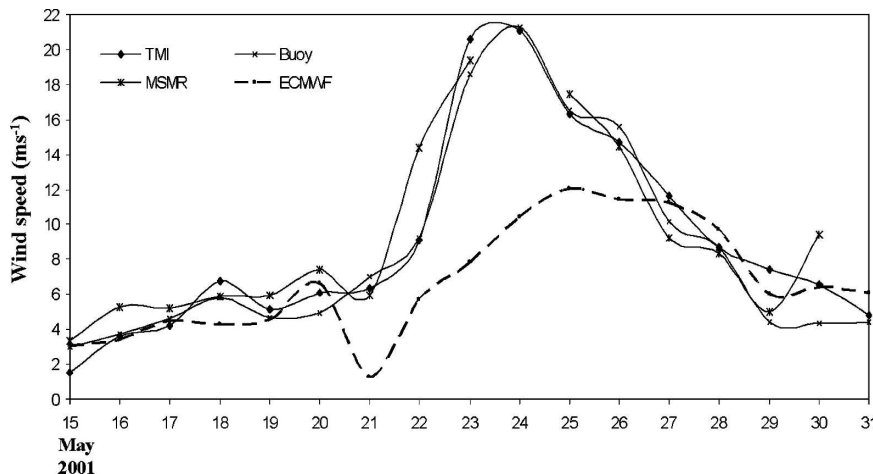


FIG. 13. Wind speed observations from buoy, TMI, MSMR, and ECMWF under the cyclonic condition at the DS1 buoy location over the Arabian Sea during 15–31 May 2001.

- satellite altimeter measurements. *J. Geophys. Res.*, **95**, 2857–2870.
- Gohil, B. S., A. K. Mathur, and A. K. Varma, 2000: Geophysical parameter retrieval over global oceans from IRS-P4/MSMR. *Proc. Fifth Pacific Ocean Remote Sensing Conf. (PORSEC 2000)*, Goa, India, NIO, 207–211.
- Gower, J. F. R., 1996: Intercalibration of wave and wind data from TOPEX/POSEIDON and moored buoys off the west coast of Canada. *J. Geophys. Res.*, **101**, 3817–3829.
- Grassl, H., 1976: The dependence of the measured cool skin of the ocean on wind stress and total heat flux. *Bound.-Layer Meteor.*, **10**, 465–474.
- Harrison, D. E., and G. A. Vecchi, 2001: January 1999 Indian Ocean cooling event. *Geophys. Res. Lett.*, **28**, 3717–3720.
- Hollinger, J. P., 1971: Passive microwave measurements of sea surface roughness. *IEEE Trans. Geosci. Electron.*, **GE-9**, 165–169.
- Hwang, P. A., W. J. Teague, G. A. Jacobs, and D. W. Wang, 1998: A statistical comparison of wind speed, wave height, and wave period from satellite altimeters and ocean buoys in the Gulf of Mexico region. *J. Geophys. Res.*, **103**, 10 451–10 468.
- Kummerow, C., W. Barnes, T. Kozu, J. Shiue, and J. Simpson, 1998: The Tropical Rainfall Measuring Mission (TRMM) sensor package. *J. Atmos. Oceanic Technol.*, **15**, 809–816.
- Liebe, H. J., 1985: An updated model for millimetre wave propagation in moist air. *Radio Sci.*, **20**, 1069–1089.
- Mears, C. A., D. K. Smith, and F. J. Wentz, 2001: Comparison of Special Sensor Microwave Imager and buoy-measured wind speeds from 1987 to 1997. *J. Geophys. Res.*, **106**, 11 719–11 729.
- Misra, T., A. M. Jha, D. Putervu, J. Rao, D. B. Dave, and S. S. Rana, 2002: Ground calibration of Multifrequency Scanning Microwave Radiometer (MSMR). *IEEE Trans. Geosci. Remote Sens.*, **40**, 504–508.
- Muraleedharan, P. M., T. Pankajakshan, and M. Harikrishnan, 2004: Validation of multi channel scanning microwave radiometer on-board Oceansat-I. *Curr. Sci.*, **87**, 370–376.
- Parekh, A., V. Bhat, and A. Sarkar, 2002: A comparative assessment of space-borne wind sensors data for an Arabian Sea cyclone. *Proc. TROPMET-2002*, Bhubneshwar, India, Indian Meteorological Society, 78–83.
- , A. Sarkar, S. Shah, and M. S. Narayanan, 2004a: Low period variability in Tropical Rainfall Measuring Mission Microwave Imager measured sea surface temperature over the Bay of Bengal during summer monsoon. *Curr. Sci.*, **87**, 791–796.
- , —, and R. Sharma, 2004b: A study of seasonal variability of sub-skin and bulk temperature over the Arabian Sea with in-situ data. *Proc. METOC*, Kochi, India, School of National Oceanology and Meteorology, and Cochin University of Science and Technology, 95–101.
- Premkumar, K. M., M. Ravichandran, S. R. Kalsi, D. Sengupta, and S. Gadgil, 2000: First results from a new observational system over the Indian Seas. *Curr. Sci.*, **78**, 323–330.
- Price, J. F., R. A. Weller, and R. Pinkle, 1986: Diurnal cycling: Observations and models of the upper ocean response to diurnal heating cooling and wind mixing. *J. Geophys. Res.*, **91**, 8411–8427.
- Quartly, G. D., J. D. Harle, M. A. Srokosz, and T. H. Guymer, 2001: Analysis of brightness temperature from the MSMR. Southampton Oceanography Centre Internal Rep. 76, 24 pp.
- Sarkar, A., S. Basu, A. K. Varma, and J. Kshatriya, 2002: Auto-correlation analysis of ocean surface wind vector. *Proc. Ind. Acad. Sci. Earth Planet. Sci.*, **111**, 297–303.
- , A. Parekh, and M. S. Narayanan, 2004: Variability of TMI derived SST in the north Indian Ocean under varying wind regimes. *Extended Abstracts, Second TRMM Int. Science Conf.*, Nara, Japan.
- Schlüssel, P., W. J. Emery, H. Grassl, and T. Mammen, 1990: On the bulk-skin temperature difference and its impact on satellite remote sensing of sea surface temperature. *J. Geophys. Res.*, **95**, 13 341–13 356.
- Senan, R., D. S. Anith, and D. Sengupta, 2001: Validation of SST and wind speed from TRMM using north Indian Ocean moored buoy observations. Indian Institute of Science Tech. Memo. CAOS Rep. 2001 AS1, 29 pp.
- Sengupta, D., B. N. Goswami, and R. Senan, 2001: Coherent intraseasonal oscillations of ocean and atmosphere during the Asian Summer Monsoon. *Geophys. Res. Lett.*, **28**, 4127–4130.
- Sharma, R., K. N. Babu, A. K. Mathur, and M. M. Ali, 2002: Identification of large-scale atmospheric and oceanic features from IRS-P4 multifrequency scanning microwave radiometer: Preliminary results. *J. Atmos. Oceanic Technol.*, **19**, 1127–1134.
- Stogryn, A., 1972: The emissivity of sea foam at microwave frequencies. *J. Geophys. Res.*, **77**, 1658–1666.
- Varma, A. K., R. M. Gairola, A. K. Mathur, B. S. Gohil, and V. K. Agarwal, 2000: Intercomparison of IRS-P4-MSMR derived geophysical products with DMSP-SSM/I, TRMM-TMI and NOAA-AVHRR finished products. *Proc. Fifth Pacific Ocean Remote Sensing Conf. (PORSEC 2000)*, Goa, India, NIO, 192–196.
- Vecchi, G. A., and D. E. Harrison, 2002: Monsoon breaks and subseasonal sea surface temperature variability in the Bay of Bengal. *J. Climate*, **15**, 1485–1493.
- Weller, R. A., M. F. Baumgartner, S. A. Josey, A. S. Fischer, and J. C. Kindle, 1998: Atmospheric forcing in the Arabian Sea during 1994–1995: Observations and comparisons with climatology and models. *Deep-Sea Res. II*, **45**, 1961–1999.
- Wentz, F. J., 1998: Algorithm theoretical basis document: AMSR ocean algorithm. Remote Sensing System Tech. Rep. 110398, 65 pp.
- , C. Geneteman, D. Smith, and D. Chelton, 2000: Satellite measurements of sea surface temperature through clouds. *Science*, **288**, 847–850.
- , P. D. Ashcroft, and C. L. Gentemann, 2001: Post launch calibration of the TMI microwave radiometer. *IEEE Trans. Geosci. Remote Sens.*, **39**, 415–422.
- Wilheit, T. T., 1979: A model for the microwave emissivity of the ocean's surface as a function of wind speed. *IEEE Trans. Geosci. Electron.*, **4**, 244–249.